IMPACT OF ANALYSIS UNCERTAINTY UPON

REGIONAL ATMOSPHERIC MOISTURE FLUX

Muyin Wang and Jan Paegle
Department of Meteorology
University of Utah, Salt Lake City, Utah 84112

December 1994

Revised May 1995

Corresponding author: Jan Paegle, Department of Meteorology, 819WBB, University of Utah,
Salt Lake City, UT 84112

/·////·˰
/N-47-CR
OCIT
63080
P· 35

ABSTRACT

Horizontal fluxes of atmospheric water vapor are studied for summer months during 1989 and 1992 over North and South America based on analyses from European Centre for Medium Range Weather Forecasts, US National Meteorological Center, and United Kingdom Meteorological Office. The calculations are performed over 20° by 20° box-shaped mid-latitude domains located to the east of the Rocky Mountains in North America, and to the east of the Andes Mountains in South America. The fluxes are determined from operational center gridded analyses of wind and moisture. Differences in the monthly mean moisture flux divergence determined from these analyses are as large as 7 cm/month precipitable water equivalent over South America, and 3 cm/month over North America. Gridded analyses at higher spatial and temporal resolution exhibit better agreement in the moisture budget study. However, significant discrepancies of the moisture flux divergence computed from different gridded analyses still exist. The conclusion is more pessimistic than Rasmusson's (1968) estimate based on station data.

Further analysis reveals that the most significant sources of error result from model surface elevation fields, gaps in the data archive, and uncertainties in the wind and specific humidity analyses. Uncertainties in the wind analyses are the most important problem. The low-level jets, in particular, are substantially different in the different data archives. Part of the reason for this may be due to the way the different analysis models parameterize physical processes affecting low-level jets. The results support the inference that the noise/signal ratio of the moisture budget may be improved more rapidly by providing better wind observations and analyses than by providing better moisture data.

1 INTRODUCTION

Water vapor is a relatively minor constituent of the earth's atmosphere but a major factor in atmospheric energetics, radiation, and transport and conversion of latent heat. Its variability and anomalies determine drought and flood episodes, and consequently modulate basic elements of the regional climate. Although the importance of atmospheric water vapor is well-recognized, its temporal and spatial variability has been systematically explored only in relatively restricted regions.

Many earlier studies of the water budget were based on subsets of the approximately 800 stations compiled within the Massachusetts Institute of Technology (MIT) General Circulation Data Library under the direction of V. P. Starr. These data consist of radiosonde soundings analyzed at 50 mb intervals over the northern hemisphere and tropical portions of the southern hemisphere for the period May 1958 - April 1963.

Rosen et al. (1979) used this data set to investigate yearly averages of vertically integrated precipitable water, and zonal and meridional atmospheric water vapor transport for a five year period and discovered substantial interannual variations. Rosen and Omdayo (1981) studied the flux of water vapor across the coastlines of the Northern Hemisphere for composite seasons of the station data. The zonal average of these fluxes is directed toward the land in the tropics, but towards the sea in some higher latitude belts.

A series of investigations by Rasmusson (1966a, 1966b, 1967 and 1968) utilized the same data set but focused upon the water transport over North America. Rasmusson (1967) investigated atmospheric water vapor fluxes in more detail over North America, and confirmed the importance of the diurnal cycle and emphasized the relevance of the southerly low-level jet located east of the Rocky Mountains for the moisture balance. Rasmusson (1968) points out that a complete hydrological cycle is difficult to define because evapotranspiration and changes in ground storage of water are largely unknown, yet he was able to obtain estimates for evaporation-precipitation (E-P) based upon the horizontal flux divergence of the atmospheric moisture using the five year data

set of the MIT Data Library. It is shown that the diurnal variations of the flux divergence are on the same order of magnitude as the computed mean flux divergence. Integration of the flux divergence fields over sufficiently large regions reduced the random components of the error (Rasmusson, 1966b), and good results can be obtained for areas about 20×10^5 km^2 and larger. Horizontally integrated maps of atmospheric flux divergence were used as proxies for E-P, together with streamflow data to compute soil storage over southern Canada and the USA. Application of this analysis to the Central Plains and Eastern United States led to an estimate of the horizontal flux divergence of water vapor that is accurate to within 0.5 cm/month precipitable water equivalent in summer.

More recent studies have used gridded analyses produced by methods of four-dimensional data assimilation (4DDA). Roads et al. (1994) performed a comprehensive study of the US. hydrologic cycle. The analysis also included station observations of precipitation, as well as streamflow, surface evaporation, and atmospheric moisture flux computed using gridded US National Meteorological Center (NMC) wind and humidity analyses produced by 4DDA. Matsuyama et al. (1994) used gridded analyses of European Centre for Medium Range Weather Forecasts (ECMWF) to study the water budget in the vicinity of the Congo River Basin in Africa, and Matsuyama (1992) compares the atmospheric flux convergence of water vapor to river discharge in the Amazon Basin. The latter study concludes that atmospheric inflow needs to be multiplied by 1.37 to match river outflow.

The conclusions of each of the aforementioned studies are affected by their estimates of atmospheric moisture flux convergence. In principle, this portion of the water cycle is the simplest to estimate, since it requires only the measurement of atmospheric wind and moisture that can be done with sufficient accuracy with radiosonde instruments. From a viewpoint emphasizing instrument technology, this requirement is less demanding than are estimates of ground storage, subsurface flow, surface evaporation, and precipitation, each of which generally require much higher resolution observations or instruments with even less coverage and heritage than the radiosonde. In practice, however, large areas of the world lack the necessary radiosonde coverage

in space and/or time to adequately describe the atmospheric component of the water cycle and current methods of 4DDA may be of questionable value in filling the gaps. Furthermore, moisture fields are often present on smaller scales than those resolved by the gridded data, and gridded values seldom represent an accurate grid box average.

The goal of the present research is to provide estimates of the variability due to differences in assimilation models of the atmospheric component of the water cycle as obtained from gridded, assimilated data. Our approach is to use different gridded analyses produced by separate, equally credible methods of 4DDA within advanced operational weather prediction centers. Moisture fluxes and flux convergences are computed from the gridded wind and moisture analyses over domains whose size is similar to large river basins. Such calculations may or may not be reliable when the separate analyses produce similar results. They are certainly questionable when different equally credible data sources produce substantial differences in the analyzed moisture flux.

The present computations of vertically integrated atmospheric water vapor flux are done on 20° x 20° boxes shown in Fig. 1. Two representative areas were selected in the current study. These are: a North American sector, characterizing an observationally data rich region; and a South American sector characterizing an observationally data poor region. The North American sector includes most of the Great Plains. The South American sector is located just south of the Amazon Basin. These regions are selected because they both have a nocturnal low level jet east of the mountains, which can be affected by the low diurnal resolution in observations as well as analyses.

Section 2 describes the data sets and Section 3 presents the atmospheric portion of the water budget over the Amazon Basin (an observationally poor region) and the Mississippi Basin (an observationally rich region). Section 4 isolates the contributions to the moisture flux uncertainty due separately to wind and moisture analysis uncertainty. Section 5 describes analyzed amplitudes of diurnal cycles in the moisture budget and relates these to diurnal cycles of the boundary layer wind. Conclusions are summarized in Section 6.

2 CALCULATION METHOD

The vertically integrated atmospheric water vapor content, W is defined as

$$W = \frac{1}{g} \int_{P_0}^{P_s} q \, dp, \tag{1}$$

where q is specific humidity, g is acceleration of gravity. Atmospheric pressures at the top level and surface are $p_0=300$ mb and $p_s=1000$ mb, respectively. The atmospheric water vapor decreases rapidly with height, and Hastenrath (1966) suggests that the 300 mb level is sufficiently high that the error due to neglect of higher levels is negligible.

The vertically integrated horizontal water vapor flux, $\bar{Q}$, is defined by

$$\bar{Q} = \frac{1}{g} \int_{P_0}^{P_s} \bar{V}q \, dp, \tag{2}$$

where $\bar{V}$ is the horizontal wind vector. The time and space average of the vertically integrated flux divergence over an arbitrary atmospheric volume overlaying a surface area A, is written as:

$$\left\langle \overline{\nabla \cdot \bar{Q}} \right\rangle = \left\langle \overline{E-P} \right\rangle - \left\langle \overline{\frac{\partial W}{\partial t}} \right\rangle. \tag{3}$$

Here the overbar denotes time mean, and angled brackets denote spatial average. The left hand side of (3) can also be computed from

$$\left\langle \overline{\nabla \cdot \bar{Q}} \right\rangle = \frac{1}{A} \oint_{perimeter \, of \, A} \bar{\bar{Q}} \cdot \bar{n} \, dL, \tag{4}$$

where L represents the curve bounding the area A, and $\bar{n}$ is the outward unit vector normal.

Direct measurements of evapotranspiration are not made and the estimate of this quantity requires high frequency surface observations of turbulent moisture and vertical velocity perturbations, available only in restricted regions of specialized surface observations. The vertical motion of the atmosphere is not directly observed on synoptic and climate time scales by the current observing system. The values of E and vertical motion that are available in gridded data sets are products of the assimilation model. These are highly sensitive to the model assumptions, and have questionable value.

By contrast, dynamical explanations of drought and flood which are related to modifications of $\bar{Q}$ and divergence of $\vec{Q}$ ($\nabla \cdot \vec{Q}$) are in principle verifiable because they require only the measurement of atmospheric wind and moisture. Early studies (e.g. Rasmusson, 1968) suggest that the reliability of the horizontal atmospheric moisture flux convergence over data rich regions of the dimension of the Mississippi river basin is on the order of 0.5 cm/month liquid water equivalent. Calculations reported here emphasize monthly periods, on domains that have dimensions approximately similar to those of the Mississippi river basin in order to facilitate comparisons with Rasmusson's (1968) reliability estimates based on station data.

The data sets include recent archives of the NMC and ECMWF for summer 1989. The data characteristics for these archives are summarized in Table 1, and are typical of the density and character of archives used in past diagnostic studies with assimilated data. The analysis methods at operational centers are frequently updated, and particularly important enhancements took place shortly after 1989. These included higher resolution boundary layer treatments and more complete surface specifications, and archives contain surface pressure. The present study includes diagnoses of $\bar{Q}$ and its divergence in more recent NMC and United Kingdom Meteorological Office (UKMO) analyses taken from summer 1992 to evaluate the impact of analysis refinements. Table 1 also summarizes the characteristics of these archives.

Moisture flux ($\vec{Q}$) and its divergence are computed from these data using the trapezoidal rule in the vertical to approximate line integrals. In these approximations, a grid point value represents the atmospheric value for a grid interval centered at the point in the approximations, and the vertical integration extends from 1000 mb to 300 mb in the 1989 archives and from the given surface pressure to 300 mb in the 1992 archives.

3. MOISTURE FLUX AND FLUX CONVERGENCE

Figure 2 displays time series of moisture flux convergence for selected months of each of the subdomains depicted in Fig. 1 for 1989 NMC and ECMWF analyses. The results for other months are similar, and not shown. The North American comparison of Fig. 2a shows that the

ECMWF and NMC results have approximately similar temporal variations on synoptic time scales. There is even approximate agreement on the diurnal time scale, as depicted by the high frequency, "saw-tooth" pattern that is especially conspicuous during the first 10 days. The monthly average appears to be small compared to the peaks, and not much larger than the magnitude of the diurnal fluctuations. The ECMWF analysis (dashed curve) produces slightly stronger convergence, or reduced divergence on most days. This appears to be a consequence of stronger inflow through the western boundary which may be affected by the presence of topography.

The time averaged discrepancy is more evident over South America (Fig. 2b). Here, there is again some similarity in the variations of the moisture flux on synoptic time scales, but less similarity on diurnal time scales, possibly because most South American radiosondes are launched only once a day, while most North American radiosondes are launched twice a day.

Figure 3 is a box diagram of the flux ($\bar{Q}$) of water vapor integrated over each lateral boundary of subdomains depicted in Fig. 1 averaged over the months selected in the time series of Fig. 2. The numbers are scaled by 10^8 kg/s, and a value of 1 corresponds to a flux sufficiently large to change the water vapor over a 4×10^6 km^2 region by approximately 6 cm liquid equivalent over one month. Numbers below and to the right of each box depict the total flux convergence.

The monthly averaged flux convergence discrepancy over the North American sector (Fig. 3a) is on the order of 0.57×10^8 kg/s, corresponding to 3.4 cm/month liquid equivalent, and it is about twice this, corresponding to 7.1 cm/month liquid equivalent over the South American sector (Fig 3b). The analysis discrepancy in the other months of this summer is similar, or slightly less than that depicted in Fig 3a, b. The results suggest that the enhanced observational density of North America produces more consistent estimates of monthly averaged moisture flux convergence than is the case for South America. There are substantial disagreements over both continents on the western boundary, perhaps due to the differing treatments of topography in the two analyses. The analysis times available for these comparisons (0000 and 1200 UTC) correspond to approximately 20:00 and 08:00 over the South American region, and 18:00 and 06:00 for the North American region. The South American times do not correspond to the time of nocturnal

low-level jet maximum, which provides an important analysis problem.

In general, the ECMWF and NMC results show substantial discrepancies. These discrepancies are significantly larger than those that could be anticipated from Rasmusson's (1968) study over the data rich North American sector. Since the largest flux differences occur on the western boundaries of the continental subdomains (Fig. 3), a significant part of the discrepancy over North and South America may be attributed to differences in model topography, together with the assumption of a bottom boundary at 1000 mb, and availability of only two analyses per day. Our experience (Paegle and Vukicevic, 1987b) with the low level jet simulations is that they differ more in their nocturnal states than day phase so that the analysis discrepancies may be more serious in analyses that include the nocturnal phase. This is the case of the North American example of Fig. 3a compared to the South American example of Fig. 3b.

More recent gridded analyses taken from NMC and UKMO archives for 1992 are available 4 times per day (instead of twice a day as in the 1989 archives); surface pressures are given (they were only partly available in the previous archives); and there is better vertical and horizontal resolution, allowing more accurate spatial integration. These improvements in the analyses produce better agreement in the moisture budget calculation shown in Fig. 4, which displays results for summer months of 1992. The North American example (Fig. 4a) shows 0.2×10^8 kg/s discrepancy (about 1.2 cm/month liquid equivalent), while the South American example of Fig. 4b produces 0.4×10^8 kg/s discrepancy (about 2.4 cm/month liquid equivalent). These results have approximately half the uncertainty of earlier comparisons shown in panels a and b of Fig. 3, but they are still worse than could be expected from Rasmusson's (1968) analysis.

4. SOURCES OF DISCREPANCY

The differences in the atmospheric moisture budget produced by different 4DDA methods are due in part to disagreement in the moisture analyses, and in part to differences in the wind analyses. There is also a possibility that, over land, they may be produced by differences in the location of the surface. The 1992 comparisons use data sets archived at rather different vertical

resolutions, and the interpolation of these may also contribute to analysis differences.

Figure 5a plots the time evolution of the normalized rms value of the meridional wind differences between NMC and ECMWF analyses at 850 mb for February 1989 along the northern inflow boundary of the South American sector. The normalization is performed through division by the rms magnitude of this wind component on this boundary averaged between the two analyses, as given by:

$$RMS\ ratio\ =\ \frac{\left[\frac{1}{N}\sum_{i=1}^{N}(X1_i - X2_i)^2\right]^{\frac{1}{2}}}{\left[0.5\times\left(\frac{1}{N}\sum_{i=1}^{N}(X1_i)^2 + \frac{1}{N}\sum_{i=1}^{N}(X2_i)^2\right)\right]^{\frac{1}{2}}}.$$

where X1 and X2 represent the selected fields from the two analyses (either the meridional wind component, or the specific humidity along the inflow boundary). The subscript i denotes the grid point, and N is the total number of grid points along the boundary. The non-dimensional ratio is plotted on the ordinate against observation time. The ratio, which is a measure of the noise/signal of the wind field on the inflow boundary is generally larger than 0.5 and occasionally exceeds 1 during February 1989. By contrast, the same noise/signal estimate of the 850 mb specific humidity on the northern inflow boundary is often around 0.2, and rarely exceeds 0.3 (Fig. 5b). The monthly averaged ratios yield 0.89 for wind (Fig. 5a) and 0.25 for specific humidity (Fig. 5b). Similar calculations over the southern inflow boundary of the North American domain produce monthly averaged 850 mb noise/signal ratios of 0.61 for the wind (Fig. 5c) and 0.20 for the moisture (Fig. 5d).

Clearly the uncertainty of the wind analysis is more critical than the uncertainty of the moisture analysis to the regional moisture budget for the 1989 analyses. This conclusion was also confirmed by switching the wind analyses of the two archives, and then switching the moisture analyses, and recalculating the moisture budget for each switched case. In all cases (results not shown), the budgets with switched moisture fields resembled the original budgets, and budgets computed with switched wind fields differed greatly from the original budgets.

Figure 6 displays noise/signal ratios similar to those of Fig. 5, computed from UKMO,

NMC analyses for February and July 1992. Over the northern inflow boundary of the South American region (Figs. 6a, 6b) monthly averaged noise/signal ratios are .63 for the wind and .4 for the specific humidity. The corresponding ratios over the southern inflow boundary of the North American region (Figs. 6c and 6d) are .33 for the wind and .16 for the specific humidity. Wind analyses show substantially better agreement than in the earlier ECMWF and NMC analyses, but the relative uncertainty in the wind analysis is significantly larger than the uncertainty in the moisture. These results support the inference that the noise/signal ratio of the moisture budget may be improved more rapidly by providing better wind observations and analyses than by providing better moisture data.

Table 2 displays the sensitivity of the calculation to the different surface pressure and the different number of archive times. This table presents the zonal flux below 775 mb through the western boundary of each domain. This boundary is the only location where the surface pressure differed by more than 10 mb between the two analyses. The first and third columns of the table are results based on UKMO and NMC analyses, respectively. The results of the second column are obtained by using the UKMO wind and moisture analyses, but starting the vertical integral from the surface pressure level given by NMC analyses. In contrast, the fourth column gives the results of calculations based on NMC wind and moisture analyses, but UKMO surface pressure analyses.

The similarity between the first and second columns, and the third and fourth columns indicates that the change in the surface pressure is not a dominant factor in the discrepancy of the moisture budget. The last column of Table 2 gives the monthly mean flux based on UKMO analyses, averaged over only those times when NMC archives are available. Comparing column five with column one it is clear that the biggest change occurs in July and January when there are five and four times missing, respectively. However, in all months the last column resembles the first column more closely than the third column, demonstrating that the differing archive completeness is not a major factor in the time averaged budget differences.

We conclude that a principal source of the budget discrepancy in the moisture analyses is due to wind analysis uncertainty. The differences associated with moisture analysis, surface pressure

analysis, and archive completeness are less important. Closer inspection reveals that the budget discrepancies increase at different times of day, mainly because of differences in the way the different analyses treat low-level diurnal wind oscillations. The next two sections summarize these results.

5. DIURNAL CYCLES OF MOISTURE BUDGET

Although more recent comparisons of NMC and UKMO analyses for 1992 are closer than earlier NMC, ECMWF comparisons for 1989, systematic discrepancies persist, especially in the diurnal cycles of boundary layer winds. Panels a and b of Fig. 7 show monthly averaged fluxes integrated over the four boundaries of the South American box for January 1992 at 0000 UTC and 1200 UTC, respectively. The direction of the flux reverses between 0000 UTC and 1200 UTC in both analyses on 3 walls (west, north, and east). The net flux convergence integrated around the complete boundary reverses as a consequence from outflow at 0000 UTC to inflow at 1200 UTC.

As noted by Rasmusson (1968), calculations of atmospheric moisture flux based upon only one observation per day can be greatly misleading. On the northern inflow boundary the NMC-UKMO difference of the diurnal cycle is about 0.8×10^8 kg/s, or 5 cm/month liquid water equivalent. This discrepancy is almost as great as the difference between monthly averaged NMC and ECMWF analyses for the net inflow across all four boundaries for all available times in February 1989 as shown in Fig. 3. The fluxes averaged over all analysis times (Fig. 4b) do not reflect such large discrepancies because of fortunate cancellation of similar differences at other boundaries and times. Because of the systematic differences at different times, the moisture budget is not much better determined than in the earlier 1989 analyses.

Over North America (Fig. 8) the diurnal oscillation is most conspicuous between 0000 UTC and 0600 UTC, especially on the southern boundary of the NMC analysis, which has 0.85×10^8 kg/s more influx at 0600 UTC than at 0000 UTC. The net flux divergence also displays larger discrepancies at individual times which largely cancel in the complete result of Fig. 4a.

6. DIURNAL CYCLES OF WIND FIELD

The diurnal fluctuations of moisture flux are due to diurnal oscillations of the low-level wind. The oscillations are especially evident around 850 mb. Based on January 1992 monthly averaged moisture flux the western portion of a cyclonic circulation over South-eastern Brazil reversed its direction from 0000 UTC to1200 UTC (figures are omitted). The southerly flow at 0000 UTC reverses to a northerly flow overnight as the northerly jet east of the Andes expands southward and eastward by 1200 UTC. The resulting circulation reversal is sufficiently strong to reverse the monthly averaged moisture flux on the northern boundary of the South American subdomain, as shown in Fig. 7. Qualitatively similar reversals occur between 1200 UTC and 0000 UTC in the NMC analyses (not shown), but there are substantial quantitative differences in that analysis. The differences are due mainly to differences in the meridional wind analysis at 850 mb, which peak at about 5 m/s at both 0000 UTC (Fig. 9a) and 1200 UTC (Fig. 9b) along east of the Andes. The UKMO analysis produces systematically stronger northerly flow flanking the east slope of the Andes.

Surface pressure analyses agree to within about 10 mb everywhere except over the high Andes, so these comparisons refer to very similar elevations above surface. It is likely that the systematic differences in the low-level jet (LLJ) strength are due mainly to systematic differences in the treatment of boundary layer physical processes by the assimilation models. Other summer months examined over South America produce similarly strong diurnal fluctuations (and discrepancies), but the northerly jet east of the Andes is usually sufficiently strong to produce a southwardly directed moisture flux at all times of day at 20°S.

Figure 10 displays moisture flux at 850 mb over the North American sector for UKMO analyses (panels a and b), and NMC analyses (panels c and d) for June 1992 at 0000 UTC (left) and 0600 UTC (right). The southerly nocturnal jet east of the Rockies is strongest at 0600 UTC, and this can be noted in an expansion and acceleration of the southerly flux centered on Texas during the night in both UKMO (panel b) and NMC (panel d) analyses.

Figure 11 display the UKMO-NMC meridional wind difference field at 850 mb for June

1992 at 0000 UTC (panel a) and 0600 UTC (panel b). The analysis differences at 0000 UTC are small and rarely exceed 1 m/s over the United States. This is the time of radiosonde launches over the United States, and the close agreement of the two analyses may reflect their fidelity to the observations. The agreement deteriorates at 0600 UTC (Fig. 11b) along the low-level jet, with peak differences of 1-4 m/s.

The LLJ has short memory of its earlier state(Paegle and Vukicevic, 1987a, 1987b). The differing evolution of the LLJ in the two analyses suggests that they have different treatments of those physical processes that modulate the jet. Nicollini et al. (1993) showed that the Great Plains LLJ is impacted strongly by presence or absence of precipitation. Earlier studies by Paegle and McLawhorn (1983) and McCorcle (1988) have demonstrated that the LLJ is sensitive to soil moisture type. It would be useful to study the analysis forecast systems in forecast mode as well analysis mode to determine if the spin-up to model physics tends to accentuate or reduce the water budget differences.

The analysis differences at 0000 UTC are systematically smaller over the well-observed North American sector than around the poorly observed South American sector. The agreement at 0600 UTC, which represents the most discrepant analysis time, is also better over North America than over South America (figure is not shown for South American case), implying that some memory of earlier states may be carried for 6 h between analysis times in data rich regions.

7 SUMMARY IMPLICATIONS

The recent GEWEX (Global Energy and Water Experiment) has been mounted in order to clarify the role of water vapor in climate (WCRP, 1993). The specific goals of GCIP (GEWEX Continental International Project) include a description of the water vapor budget over North America on time scales of 10-30 days. Many of the new components of the observing system for GEWEX are asynchronous with respect to the standard 0000 GMT and 1200 GMT observing times that were used in the previously cited water vapor budget experiments, and they can be adequately incorporated in the observing system only through the process of 4DDA. Data sets

produced by 4DDA are much more commonly used in current large scale diagnostics than are station data and analyses derived at standard observing times as in the case of the MIT General Circulation Data Library. The method of 4DDA has potential shortcomings which have been pointed out by many investigators. One of these is that certain key elements of the circulation deduced from observations assimilated in this fashion are more strongly dependent upon the analysis model used than upon the available observations. This has been shown by intercomparisons of different operational and research data sets by Paegle et al. (1986), Trenberth and Olson (1988) and Trenberth (1991).

The purpose of this investigation has been to present early estimates of the atmospheric portions of the hydrology cycle based upon operational data sets produced through 4DDA. One of the study regions covers the area east of the Rocky Mountains, which was studied in the series of radiosonde station data investigations by Rasmusson and is of particular concern to GCIP. Regional diagnoses of the water vapor budget for selected summer months of 1989 suggest more pessimistic conclusions for monthly averaged flux divergence estimates of the atmospheric portion of the hydrological cycle than those given by Rasmusson (1968) in the sense that NMC and ECMWF analyses produce monthly differences of the flux of water vapor that are equivalent to E-P uncertainties on the order 7 cm/month over South America, and about 3 cm/month over the eastern United States.

Other analyses using these 4DDA data sets are certainly not invalidated by our results. Roads et al., (1994), for example, corrected for problems at the poorly defined lower boundary by using available estimates of topography height. Matsuyama et al. (1992) adjusted the ECMWF divergence to conform with streamflow information. These tactics have not been used here because we simply wanted to determine how reliable the atmospheric analyses are independent of other information.

Some of these difficulties are related to problems of interpolation of the sigma level data to pressure levels (Trenberth, 1991), and to inconsistent handling of the surface pressure. The impact of these uncertainties is examined by comparing more highly resolved and physically more

complete analyses of the UKMO and the NMC for selected months of 1992. The monthly averaged results east of the Rocky Mountains are in better agreement with Rasmusson's (1968) conclusions than in the case of the 1989 analysis intercomparisons.

Closer scrutiny suggests that the relatively better results are due partly to cancellation of systematic errors that characterize the results composited at 6 hour intervals. These errors are connected more closely to uncertainties of the wind analyses than to uncertainties of the moisture analyses. In particular, the timing and location of the operational radiosonde observing system appears to be inadequate for the resolution of the diurnally oscillating LLJ. The jet and its diurnal oscillations show significant variability on synoptic and monthly time scales and these fluctuations account for much of the variability of the moisture budget and deduced E-P estimates over large regions of North and South America.

Past studies of the LLJ have shown that its structure in short-term forecasts is more sensitive to parameterization of model processes such as turbulent atmospheric mixing than to reasonable changes of initial data (Paegle and Vukicevic, 1987a, 1987b). McCorcle (1988) and Fast and McCorcle (1990) also demonstrated substantial sensitivity to soil moisture and Nicolini et al. (1993) show that there are important feedback effects from nocturnal precipitation events triggered by the LLJ. The analysis of an LLJ in a 4DDA cycle may have problems similar to those found in the analysis of the Hadley and Walker circulations in the sense that these circulations depend so sensitively upon model assumptions that even good input data may be insufficient to guarantee reliable gridded analyses. This possibility is supported by our conclusion that 4DDA generated E-P analyses show more uncertainty over the Plains and eastern United States than analyses based on station data summarized by Rasmusson (1968).

In view of this, and in view of the dependence of the E-P uncertainty upon the wind field in general, and upon the LLJ in particular, it is important to perform the diagnostics using the most advanced modeling technology available with respect to treatment of the LLJ and to calculate the budgets on the highest resolution commensurate with the assimilation model. It would be useful to study the analysis forecast systems in forecast mode as well analysis mode to determine if the spin-

up to model physics tends to accentuate or reduce the water budget differences.

REFERENCES

Fast, J. D., and M. D. McCorcle, 1990: A two-dimensional numerical sensitivity study of the great plains low-level jet. *Mon. Wea. Rev.*, **118**, 151-163.

GEWEX Cloud System Science Team, 1993: The GEWEX Cloud System Study (GCSS). *Bull of Amer. Meteor. Soc,* **74**, 387-399.

Hastenrath, S. L., 1966: The flux of atmospheric water vapor over the Caribbean sea and the gulf of Mexico. *J. of Appl. Meteor.*, **5**, 778-788.

Matsuyama, H., 1992: The water budget in the Amazon river basin during the FGGE period. *J. Meteor. Soc. Japan,* **70**, 1071-1084.

Matsuyama, H., T. Oki, M. Shinoda and K. Masuda, 1994: The seasonal change of the Congo River Basin. *J. Meteor. Soc. Japan,* **72**, 281-299.

McCorcle, M. D., 1988: Simulation of surface-moisture effects on the great plains low-level jet. *Mon. Wea. Rev.*, **116**, 1705--1720

Nicolini, M., K. M. Waldron, and J. Paegle, 1993: Diurnal oscillations of low-level jets, vertical motion, and precipitation: a model case study. *Mon. Wea. Rev.* **121**, 2588-2610.

Paegle, J. and D. W. McLawhorn, 1983: Numerical modeling of diurnal convergence oscillations above sloping terrain. *Mon. Wea. Rev.*, *111*, 67--85.

Paegle, J., W. E. Baker and J. N. Paegle, 1986: The analysis sensitivity to tropical winds from the global weather experiment. *Mon. Wea. Rew.*, **114**, 991-1007.

Paegle, J., and T. Vukicevic, 1987a: The analysis and forecast sensitivity of low-level mountain flows to input data. Preprints, *Fourth Conf. on Mountain Meteorology*, Seattle, Amer. Meteor. Soc., 168--174.

Paegle, J., and T. Vukicevic, 1987b: On the predictability of low-level flow during ALPEX. *Meteor. Atmos. Phys.*, **36**, 45--60.

Rasmusson, E. M., 1966a: Diurnal variations in the summer water vapor transport over North America. *Water Resour. Res.*, 2, 469-477.

Rasmusson, E. M., 1966b: Atmospheric water vapor transport and the hydrology of North America. *Report No. A-1*, Planetary Circulations Project, Massachussetts Institute of Technology, 170pp

Rasmusson, E. M., 1967: Atmospheric water vapor transport and the water balance of North America, Part I. characteristics of the water vapor flux field, *Mon. Wea. Rev.*, 95, 403-426.

Rasmusson, E. M., 1968: Atmospheric water vapor transport and the water balance of North America, Part II. Large-scale water balance investigations. *Mon. Wea. Rev.*, 96, 720-734.

Roads, J. O., S-C. Chen, A. K. Guetter, and K. P. Georgakakos, 1994: Large-scale aspects of the United States hydrologic cycle. *Bull. Amer. Meteor. Soc.*, 75, 1589-1610

Rosen, R. D., D. A. Salstein, and J. P. Peixoto, 1979: Variability in the annual fields of large-scale atmospheric water vapor transport. *Mon. Wea. Rev.*, 114, 2352-2362.

Rosen, R. D., and A. S. Omolayo, 1981: Exchange of water vapor between land and ocean in the northern hemisphere. *J. Geophys. Res.*, 86, 12147-12152.

Trenberth, K. E. and J. G. Olson, 1988: An evaluation and intercomparison of Global analyses from the National Meteorological Center and the European Centre for Medium Range Weather Forecasts. *Bull of Amer. Meteor. Soc.*, 69, 1047-1057.

Trenberth K. E., 1991: Climate diagnostics from global analyses: conservation of mass in ECMWF analyses. *J. of Climate*, 4, 707-722.

FIGURE CAPTIONS

Figure 1 Computational domains (boxes) of (a) North American sector and (b) South American sector. Contours show the orography based on NMC analyses. Contour interval is 250 meters.

Figure 2 Time series of moisture flux divergence over (a) North American sector for July, 1989, and (b) over South American sector for February 1989. Units in the diagram are 10^8 kg/s. Solid lines are the results obtained from NMC analyses, and dashed lines from ECMWF analyses.

Figure 3 Monthly averaged moisture flux and flux divergence for (a) North America (July 1989), and (b) South America (February 1989). Units are 10^8 kg/s. Hatched arrows indicate the results based on ECMWF analyses, and blank arrows indicate the results based on NMC analyses.

Figure 4. As in Fig. 3 for (a) June and (b) January 1992 over North and South America, respectively. Units are 10^8 kg/s. Hatched arrows indicate the results based on UKMO analyses, and blank arrows indicate the results based on NMC analyses.

Figure 5. Normalized rms ratio of analysis differences between NMC and ECMWF for 1989 case. Rms ratios of (a) wind and (b) specific humidity analyses over South American inflow boundary for February, 1989. Similarly rms ratios of (c) wind and (d) specific humidity for North American inflow boundary for July 1989.

Figure 6. As in Fig. 5 for 1992 case: (a) South America February 1992 wind analysis, (b) South America February 1992 specific humidity analyses, (c) North America July 1992 wind analyses, and (d) North America July 1992 specific humidity analyses.

Figure 7 Monthly mean moisture flux and flux convergence averaged over (a) 0000 UTC, and (b) 1200 UTC for January 1992 over South America. Hatched arrows indicate results based on UKMO analyses, and blank arrows indicate results based on NMC analyses. Units are 10^8 kg/s.

Figure 8 Monthly mean moisture flux and flux divergence averaged over (a) 0000 UTC, and (b) 0600 UTC for June 1992 over North America. Hatched arrows indicate the results based on UKMO analyses, and blank arrows indicate the results based on NMC analyses. Units are 10^8 kg/s.

Figure 9 Monthly mean 850 mb meridional wind difference between UKMO and NMC analyses averaged at (a) 0000 UTC, and (b) 1200 UTC. Negative contours are dashed. Contour interval is 1 m/s.

Figure 10 Monthly averaged moisture flux (vq dp/g) at 850 mb for North America June 1992 based on UKMO analyses, (a) and (b), and NMC analyses (c) and (d). Left panels are averaged at 0000 UTC, and right panels averaged over 0600 UTC. Contour interval is 25 kg/ms.

Figure 11 Monthly mean 850 meridional wind difference between UKMO and NMC analyses averaged at (a) 0000 UTC, and (b)0600 UTC over North America. Negative contours are dashed. Contour interval is 1 m/s.

Table 1 Archived data sets

1989 summer	NMC/ECMWF	Resolution	2.5°X2.5°
		Vert. Level	1000, 850, 700, 500, 300 mb
		Frequency	0000Z, 1200Z
		Period	Dec. 1, 1988 -- Feb. 28, 1989 Jun. 1, 1989 -- Aug. 31, 1989
	Missing data	NMC	2 times
		ECMWF	NONE
1992 summer	NMC	Resolution	1.125° X 1.125°
		Vert. Level	18 sigma levels
		Frequency	0000Z, 0600Z, 1200Z, 1800Z
		Period	Dec. 1 1991 -- Feb. 29 1992
		Missing data	13 times
	UKMO	Resolution	1.25° X 0.833°
		Vert. Level	950, 850, 700, 500, 400, 300 mb
		Frequency	0000Z, 0600Z, 1200Z, 1800Z
		Period	Dec. 1 1991 -- Feb. 29 1992
		Missing data	2 times

Table 2 Moisture fluxe through the western boundary
over North and South American sectors. (1000-775 mb) Unit: 10^8 kg/s.

		UKMO	UKMO NMC_sfp	NMC	NMC UKMO_sfp	UKMO part
South America	December	-0.3254	-0.2832	0.0393	0.0423	-0.3260
	January	-0.5401	-0.6034	-0.3590	-0.3506	-0.5560
	February	-0.4494	-0.5125	-0.0672	-0.0621	-0.4494
North America	June	-0.0468	-0.0966	-0.1023	-0.1045	-0.0526
	July	0.2233	0.1615	0.0787	0.1222	0.1994
	August	0.0151	-0.0197	-0.0305	0.0393	0.0161

60°N .... 60°N

H_647

1250

H_2997

H_700

30°N .... 30°N

H_2258

EQ -----EQ-------- EQ

H_4776

H_1055

1250

30°S ---------- 30°S

H_26

1250

H_27   H_102

H_26   H_26

60°S .... 60°S

120°W   90°W   60°W

CONTOUR FROM 250 TO 4750 BY 250

Fig. 1

Fig. 2

(a)

0.11   0.45

0.44

0.72

3.01

2.53

1.99   1.54

Total flux convergence
= -1.15 NMC   *Outflow*
= -0.58 ECMWF   *Outflow*

(b)

2.02   2.18

0.47

0.26

1.83

2.00

0.06   0.16

Total flux convergence
= -0.19 NMC   *Outflow*
= 0.99 ECMWF   *Inflow*

Fig. 3

(a)

0.07   0.12

1.58 ⟶   ⟶ 2.56

1.40 ⟶   ⟶ 2.37

1.11   1.26

Total flux convergence
= 0.20 NMC   *Inflow*
= 0.39 UKMO   *Inflow*

(b)

0.23   0.21

0.33 ⟶   ⟵ 0.14

0.21 ⟶   ⟶ 0.29

0.27   0.56

Total flux convergence
= -0.12 NMC   *Outflow*
= 0.13 UKMO   *Inflow*

Fig. 4

Fig. 5

Fig. 9.

(a)

0.48   0.97

0.06

0.85

0.39

0.13

Total flux convergence
= -0.96 NMC   *Outflow*
= -0.67 UKMO *Outflow*

0.22   0.50

(b)

0.88   1.21

0.69

0.37

0.54

0.53

Total flux convergence
= 0.64 NMC   *Inflow*
= 1.13 UKMO *Inflow*

0.25   0.40

Fig. 7

(a)

0.11   0.21

1.19

2.33

1.27

2.32

Total flux convergence
= -0.29 NMC   *Outflow*
= 0.19 UKMO *Inflow*

0.64   1.12

(b)

0.12   0.08

1.64

2.74

1.40

2.32

Total flux convergence
= 0.69 NMC   *Inflow*
= 0.45 UKMO *Inflow*

1.49   1.48

Fig. 8

UK–NMC Diff of V JANUARY   00Z 950. mb   UK–NMC Diff of V JANUARY   12Z 950. mb
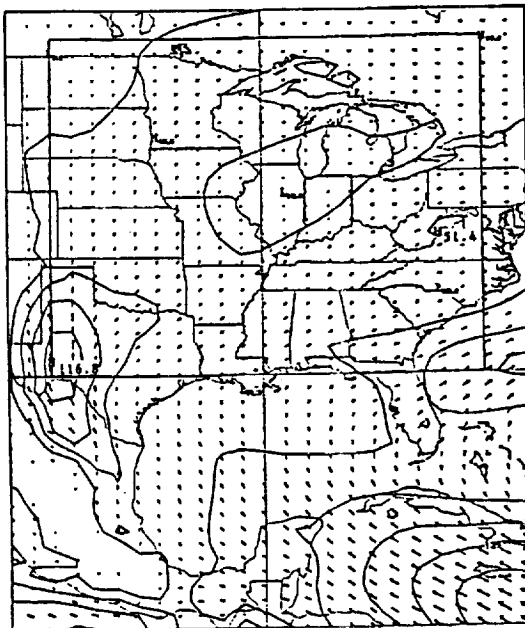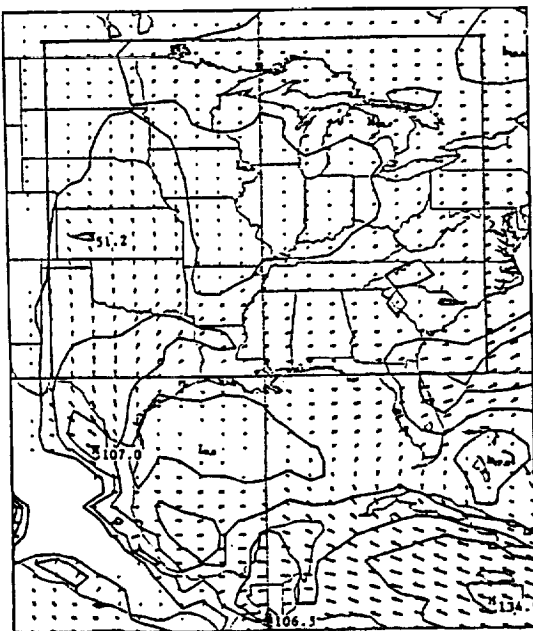
Fig. 9

UKMO   JUNE   00Z 850. mb H20 Flux   UKMO   JUNE   06Z 850. mb H20 Flux
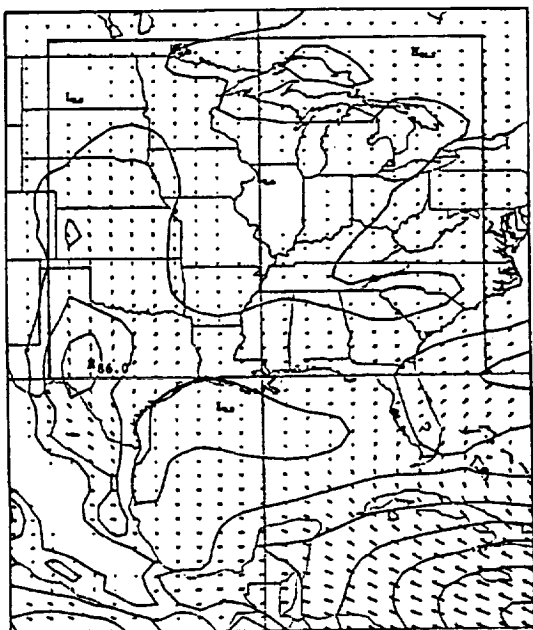
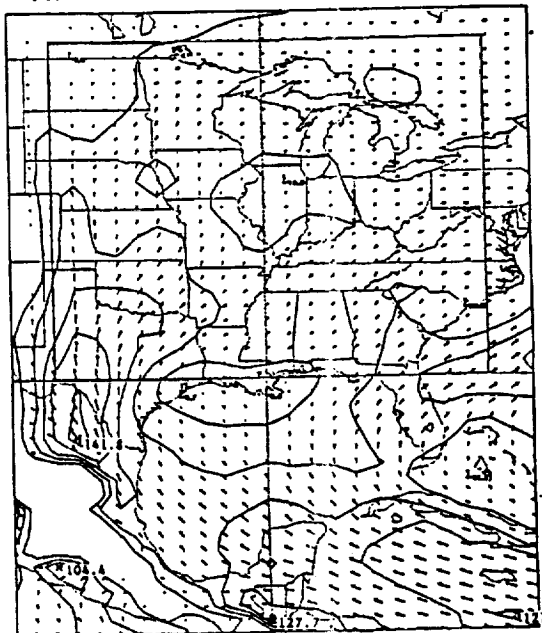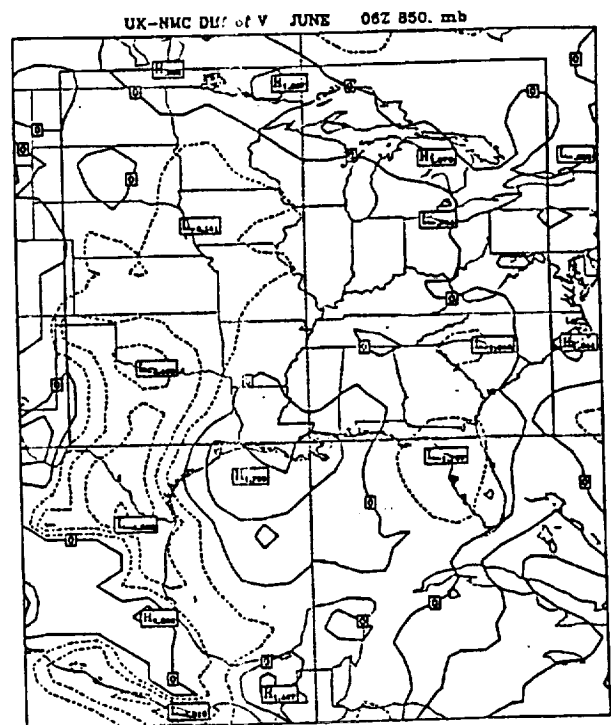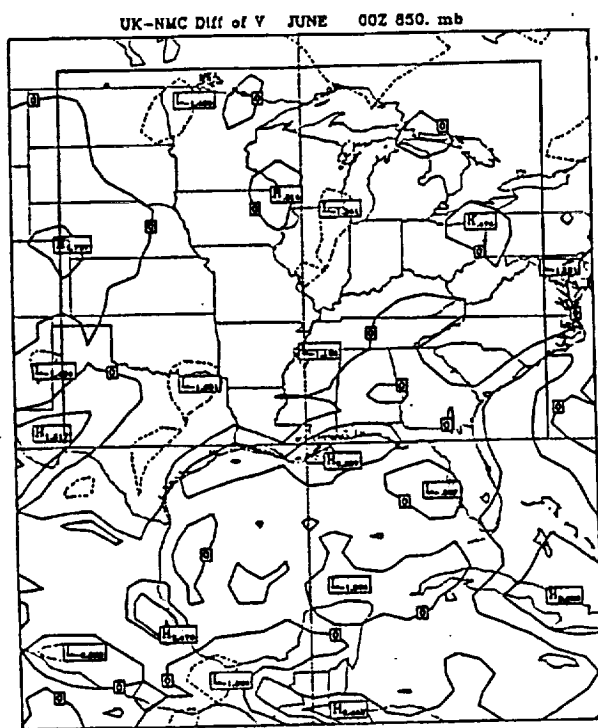NMC   JUNE   00Z 850. mb H20 Flux   NMC   JUNE   06Z 850. mb H20 Flux

Fig. 10

UK-NMC Diff of V   JUNE   00Z 850. mb

UK-NMC Diff of V   JUNE   06Z 850. mb

Fig. 11

Report Documentation Page

1. Report No.	2. Government Accession No.	3. Recipient's Catalog No.

4. Title and Subtitle		5. Report Date
Analyses and Forecosts with LAWS Winds		7-15-95
		6. Performing Organization Code
		(

7. Author(s)		8. Performing Organization Report No.
Jan Paegle		
		10. Work Unit No.

9. Performing Organization Name and Address		11. Contract or Grant No.
University of Utah Dept. of Meteorology Salt Lake City, UT 84112		512871
		13. Type of Report and Period Covered

12. Sponsoring Agency Name and Address		Final 9/22/93 – 12/31/94
National Aeronautics and Space Administration Mail Stop 126 Hampton VA, 23665		14. Sponsoring Agency Code
		P.O.# S-12871·F

15. Supplementary Notes

16. Abstract

See attached sheet.

ORIGINAL PAGE IS
OF POOR QUALITY

17. Key Words (Suggested by Author(s))		18. Distribution Statement
Space-based winds hydrologic cycle		

19. Security Classif. (of this report)	20. Security Classif. (of this page)	21. No. of pages	22. Price